arXiv:0908.0381v1 [quant-ph] 4 Aug 2009

Single mode quantum properties of the codirectional Kerr nonlinear coupler: frequency mismatch and exact solution

Faisal A. A. El-Orany,[1] M. Sebawe Abdalla,[2] and and J. Peřina[3]

[1]*Department of Mathematics and Computer Science, Faculty of Science, Suez Canal University, Ismailia, Egypt*

[2]*Mathematics Department, College of Science, King Saud University, P.O. Box 2455, Riyadh 11451, Saudi Arabia*

[3]*Department of Optics and Joint Laboratory of Optics, Palacký University, 17. listopadu 50, 772 07 Olomouc, Czech Republic*

(Dated: August 4, 2009)

In this paper, we investigate the single mode quantum properties of the codirectional Kerr nonlinear coupler when the frequency mismatch is involved and a condition for an exact solution of equations of motion is fulfilled. Particularly, we investigate quadrature and principal squeezing, Wigner function, quadrature distribution, phase distribution and phase variance. We show that the quadrature squeezing and the phase variance can exhibit collapse-revival and collapse-revival-subrevival phenomena, respectively, based on the values of the detuning parameter. Furthermore, we analytically demonstrate that the system can generate cat states, in particular, Yurke-Stoler states.

PACS numbers: 42.50Dv,42.60.Gd

Keywords: Quasiprobability functions; nonlinear coupler; squeezed light; quantum phase

I. INTRODUCTION

Recently, there has been a great interest in the possibility of using optical devices for ultra-ligh-speed data processing. This is the main object in the quantum information theory, which aims at storing and transferring data [1]. One of the promising devices for data transmission is the nonlinear directional coupler that consists of two or more parallel optical waveguides fabricated from some nonlinear material. Both waveguides are placed close enough to permit

flux-dependent transfer of energy between them by means of evanescent waves. This flux transfer can be controlled by the device design and the intensity of the input flux as well. The outgoing fields from the coupler can be examined as single or compound modes by means of homodyne detection to observe squeezing of vacuum fluctuations, or by means of a set of photodetectors to measure photon correlations, photon antibunching and sub-Poissonian photon statistics in the standard ways. The investigation of the quantum properties of light propagating in the directional couplers have attracted much attention for generating nonclassical light (see the review paper [2] and the references therein). Moreover, directional coupler is experimentally implemented, e.g. in planar structures [3], dual optical fibres [4] and certain organic polymers [5].

Among the different types of directional couplers the directional Kerr nonlinear coupler (DKNC) has taken much attention as a result of its application in optics as an intensity-dependent routing switch [6, 7]. DKNC is useful for low intensity fields and periodical exchange of energy between the guides; but for high intensity fields, energy is trapped by nonlinearity in the guide into which it was initially launched (self-trapping effect). The quantum properties of the DKNC have been studied by several authors [8, 9, 10, 11, 12, 13, 14]. For instance, in [10] quadrature squeezing, principal squeezing and integrated intensity variances have been calculated in an analytical way and investigated based on the transmission of light between waveguides. Moreover, quantum statistics for contradirectional KNC have been investigated [14] showing that the switching between waveguides is accompanied by nonclassical effects, e.g. two-mode squeezing, the generation of pure state and single mode photon antibunching. Influence of the geometry of the coupler (when the linear coupling coefficient is variable) on the statistics of the DKNC [11, 15] (also contradirectional KNC [15]) was investigated showing that there is a possibility to control energy switching between waveguides by adjusting the form of a coupling function. The numerical technique based on the diagonalization of the Hamiltonian is used for studying the mean-photon number [7] and the phase distribution in the framework of a quasiprobability distribution function [12]. Furthermore, in the most of papers dealing with DKNC in the literature, e.g. [10, 11, 12, 13, 14], authors have shown that the evolution of the mean-photon numbers exhibit collapse-revival phenomenon arising from the nonlinear exchange of energy between waveguides. In this regard there is a similarity between DKNC and the behaviour of the atomic inversion in the Jaynes-Cummings model [16]. In the present paper we provide–under

a certain condition–the exact solutions for the equations of motion of DKNC taking into account the frequency mismatch. This would lead to many important results additionally to what are already known for DKNC. For instance, we show that the quadrature squeezing can exhibit collapse-revival phenomenon rather than the mean-photon numbers, as shown earlier [7, 10, 11, 13, 14]. Also the phase variances exhibit collapse-revival-subrevival phenomenon similar to that of the two-mode Jaynes-Cummings model [17]. Moreover, for the first time, we analytically and numerically prove that the system can generate Yurke-Stoler states at certain times despite the coupling of the two modes.

Now the Hamiltonian controlling the codirectional Kerr nonlinear coupler is given as

$$\frac{\hat{H}}{\hbar} = \sum_{j=1}^{2}[\omega_j \hat{a}_j^{\dagger}\hat{a}_j + \chi \hat{a}_j^{\dagger 2}\hat{a}_j^2] + \widetilde{\chi}\hat{a}_1^{\dagger}\hat{a}_1\hat{a}_2^{\dagger}\hat{a}_2 + \kappa(\hat{a}_1^{\dagger}\hat{a}_2 + \hat{a}_2^{\dagger}\hat{a}_1), \tag{1}$$

where ω_1 and ω_2 are the frequencies of the first and the second modes with the annihilation operators $\hat{a}_1$ and $\hat{a}_2$, respectively, χ and $\widetilde{\chi}$ are the coupling constants proportional to the third-order susceptibility $\chi^{(3)}$ and responsible for the self-action and cross-action processes, respectively, κ is the linear coupling constant between the waveguides. Kerr coupler can be implemented from certain organic polymers with high third-order nonlinearities [5]. Also cento-symmetric optical fibres can be adopted. We proceed that in above mentioned papers related to DKNC, i.e. [10, 11, 12, 13, 14], the authors have neglected the non-relevant terms, i.e. the nonlinear rotational terms, for obtaining a closed form solution of the equations of motion related to (1). In this paper we restrict ourselves to the case in which the equations of motion can be solved exactly. In this case the system is linear in the sense that the mean-photon numbers exhibit oscillatory behaviour indicating periodic energy exchange between the waveguides even though there is a nonlinear medium between the waveguides. Actually, this does not mean that the coupler cannot generate nonclassical effects. More illustratively, the mean-photon numbers are given by the diagonal elements of the density matrix only. Nevertheless, the quantities, which depend on the off-diagonal elements, such as quadratures squeezing, Wigner function, phase distribution, etc., may generate nonclassical effects. Thus we are going to investigate the behaviour of these quantities in the present paper, considering also the influence of frequency mismatch $\Delta = \omega_1 - \omega_2$. It is worth remembering that the phase mismatches were considered to the other types of coupler, e.g. linear coupler [18], nonlinear coupler [19] and Raman-Brillouin couplers [20].

We conclude this section by writing the equations of motion for (1) under the condition

$\widetilde{\chi} = 2\chi$,

$$\begin{aligned}
\frac{d\hat{a}_1}{dt} &= -i\omega_1\hat{a}_1 - 2i\chi(\hat{a}_1^\dagger\hat{a}_1 + \hat{a}_2^\dagger\hat{a}_2)\hat{a}_1 - i\kappa\hat{a}_2, \\
\frac{d\hat{a}_2}{dt} &= -i\omega_2\hat{a}_2 - 2i\chi(\hat{a}_1^\dagger\hat{a}_1 + \hat{a}_2^\dagger\hat{a}_2)\hat{a}_2 - i\kappa\hat{a}_1.
\end{aligned} \tag{2}$$

One can easily check that $\hat{a}_1^\dagger\hat{a}_1 + \hat{a}_2^\dagger\hat{a}_2 = \hat{C}$ is a constant of motion and hence the general solution for (2) is

$$\begin{aligned}
\hat{a}_1(t) &= \exp(-i\hat{\Lambda}t/2)\Big\{\hat{a}_1(0)\left[\cos(\lambda t) - i\tfrac{\Delta}{2\lambda}\sin(\lambda t)\right] - i\tfrac{\kappa}{\lambda}\hat{a}_2(0)\sin(\lambda t)\Big\}, \\
\hat{a}_2(t) &= \exp(-i\hat{\Lambda}t/2)\Big\{\hat{a}_2(0)\left[\cos(\lambda t) - i\tfrac{\Delta}{2\lambda}\sin(\lambda t)\right] - i\tfrac{\kappa}{\lambda}\hat{a}_1(0)\sin(\lambda t)\Big\},
\end{aligned} \tag{3}$$

where $\lambda = \sqrt{\kappa^2 + \frac{1}{4}\Delta^2}$, $\hat{\Lambda} = \omega_1 + \omega_2 + 4\chi\hat{C}$ and Δ is the frequency mismatch. One can easily check that $\hat{a}_1(t) \leftrightarrow \hat{a}_2(t)$ when $\hat{a}_1(0) \leftrightarrow \hat{a}_2(0)$. Thus we restrict the discussion to the behaviour of the first mode only. It is worth mentioning that for solving the problem in the space domain we have to use the substitution $z = t\vartheta$, where ϑ is the velocity of light in the waveguide and z is the travelled distance. Moreover, we do not consider the dissipation, which generally leads to decrease of the total number of photons and to the tendency to reduce the exchange of photons between the waveguides, i.e. to the reduction of the nonclassical effects [8, 9].

Finally, using (3) we investigate only the single mode quantum properties for the DKNC. We perform such investigation in the following order: In section 2 we examine the quadratures and principal squeezing. In section 3 we calculate and discuss the quasiprobability distribution and quadrature distribution. In section 4 we study the phase distribution and its variance. The results are summarized in section 5.

II. QUADRATURES AND PRINCIPAL SQUEEZING

The photons produced in a nonlinear optical device such as DKNC are known to have unusual correlation properties, which results in many nonclassical aspects of the radiation field. Thus in this section we demonstrate the single mode quadratures and principal squeezing. As is well known squeezed light has less noise than coherent light in one of the field quadratures. This light can be measured by homodyne detection where the signal is superimposed on a strong coherent beam of the local oscillator. Moreover, squeezing is one of the

most important phenomenon in quantum optics because of its applications in various areas, e.g., in optics communication, quantum information theory, etc.[21].

To investigate the single mode squeezing we define two quadratures $\hat{X}$ and $\hat{Y}$, which denote the real (electric) and imaginary (magnetic) parts, respectively, of the radiation field, as

$$\hat{X} = \frac{1}{\sqrt{2}}[\hat{A}_1(t) + \hat{A}_1^\dagger(t)], \quad \hat{Y} = \frac{1}{i\sqrt{2}}[\hat{A}_1(t) - \hat{A}_1^\dagger(t)], \tag{4}$$

where $\hat{A}_1(t) = \hat{a}_1(t)\exp[\frac{it}{2}(\omega_1+\omega_2)]$. As we mentioned in section 1 we restrict the discussion to the first mode. The quadrature operators (4) satisfy the following commutation relation

$$\left[\hat{X}, \hat{Y}\right] = i. \tag{5}$$

Therefore, the uncertainty relation related to (5) is

$$\langle(\triangle\hat{X})^2\rangle\langle(\triangle\hat{Y})^2\rangle \geq \frac{1}{4}, \tag{6}$$

where the variance $\langle(\triangle\hat{X})^2\rangle = \langle\hat{X}^2\rangle - \langle\hat{X}\rangle^2$ and similarly form can be given for $\langle(\triangle\hat{Y})^2\rangle$. We say that the system exhibits X-quadrature squeezing when

$$S = 2\langle(\triangle\hat{X}(t))^2\rangle - 1 \leq 0. \tag{7}$$

The equality sign holds, i.e. $S = 0$, for minimum-uncertainty states. Similar definition can be given for the Y-quadrature (defining a Q-factor).

On the other hand, the quadratures (4) can be represented by the Hermitian operator

$$\hat{V}_\phi = \frac{1}{\sqrt{2}}[\hat{A}_1(t)\exp(-i\phi) + \hat{A}_1^\dagger(t)\exp(i\phi)], \tag{8}$$

where ϕ is a phase, which can be controlled by the homodyne detector. The operator (8) reduces to the X-quadrature (the in-phase component of the field) when $\phi = 0$, while when $\phi = \pi/2$, it gives the Y-quadrature (out-of-phase component of the field). According to (8) the variance is dependent on the phase ϕ, which can be controlled to give the minimum of all quadrature variances [22, 23]. Thus we obtain the notion of the principal squeezing [22, 23], which can be expressed for the single-mode as

$$\eta(t) = 2[\langle\hat{A}_1^\dagger(t)\hat{A}_1(t)\rangle - \langle\hat{A}_1^\dagger(t)\rangle\langle\hat{A}_1(t)\rangle - |\langle\hat{A}_1^2(t)\rangle - \langle\hat{A}_1(t)\rangle^2|]. \tag{9}$$

Squeezing occurs when $\eta(t) < 0$.

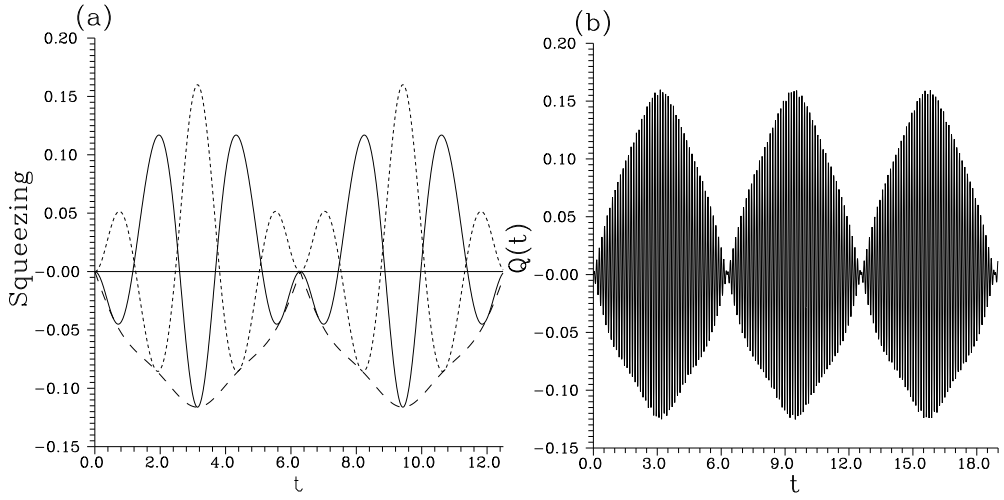

FIG. 1: Evolution of the squeezing factors and principal squeezing of the first mode when $\kappa = 1, \chi = 0.5, (\alpha_1, \alpha_2) = (0.2, 0.2)$ and for (a) $\Delta = 0s^{-1}$ (solid curve for $S(t)$, short-dashed curve for $Q(t)$ and long-dashed curve for $\eta(t)$), (b) evolution of the factor $Q(t)$ for $\Delta = 50s^{-1}$. The straight line in (a) is given to show the squeezing bound.

The different moments of the operator $\hat{A}_1(t)$ can be evaluated as

$$\langle \hat{A}_1^{\dagger m}(t)\hat{A}_1^n(t)\rangle = \bar{\alpha}_1^n(t)\bar{\alpha}_1^{*m}(t)z^{[\frac{n}{2}(n-1)-\frac{m}{2}(m-1)]}\exp[\varepsilon(z^{n-m}-1)], \tag{10}$$

where

$$\varepsilon = |\alpha_1|^2 + |\alpha_2|^2, \quad z = \exp(-2i\chi t), \quad \bar{\alpha}_1(t) = \bar{\alpha}_x(t) + i\bar{\alpha}_y(t) \tag{11}$$

and

$$\bar{\alpha}_x(t) = \alpha_1\cos(\lambda t), \quad \bar{\alpha}_y(t) = -[\alpha_1\frac{\Delta}{2} + \alpha_2\kappa]\frac{\sin(\lambda t)}{\lambda}, \tag{12}$$

where α_1 and α_2 are the initial field amplitudes. Throughout the paper we consider that α_1 and α_2 are real. Expression (10) reflects two facts: (i) When $\chi = 0$ the system reduces to the up conversion process, which switches the energy between the waveguides without generating nonclassical effects. (ii) When $n = m$ all the moments are independent of χ and the mean-photon numbers exhibit oscillatory behaviour only rather than collapse-revival pattern, which is representative for the DKNC [9, 10, 11, 12, 13, 14]. Moreover, this fact shows that the system exhibits always Poissonian statistics.

Now we start the discussion by investigating the behaviour of the quadratures squeezing. We show that the system can provide squeezing and the quadrature squeezing can exhibit the collapse-revival phenomenon. Furthermore, squeezing cannot be simultaneously generated

in the two quadratures. In doing so we use (10) to express the squeezing factors $S(t)$ and $Q(t)$ as

$$\begin{aligned} S(t) &= 2|\bar{\alpha}_1(t)|^2 + G_1(t) - G_2(t), \\ Q(t) &= 2|\bar{\alpha}_1(t)|^2 - G_1(t) - G_3(t), \end{aligned} \tag{13}$$

where

$$\begin{aligned} G_1(t) &= 2[(\bar{\alpha}_x^2(t) - \bar{\alpha}_y^2(t))\cos(\epsilon(2\chi t)) + 2\bar{\alpha}_x(t)\bar{\alpha}_y(t)\sin(\epsilon(2\chi t))]f(2\chi t), \\ G_2(t) &= 4[\bar{\alpha}_x(t)\cos(\epsilon(\chi t)) + \bar{\alpha}_y(t)\sin(\epsilon(\chi t))]^2 f^2(\chi t), \\ G_3(t) &= 4[\bar{\alpha}_x(t)\sin(\epsilon(\chi t)) - \bar{\alpha}_y(t)\cos(\epsilon(\chi t))]^2 f^2(\chi t), \\ \epsilon(n\chi t)) &= n(n-1)\chi t + \varepsilon\sin(2n\chi t), \\ f(n\chi t) &= \exp[-2\varepsilon\sin^2(n\chi t)]. \end{aligned} \tag{14}$$

It is obvious that the behaviours of $S(t)$ and $Q(t)$ are periodic as a result of the nature of the coupler, which basically depends on switching energy between waveguides by means of the evanescent waves. Moreover, the origin of the occurrence of the nonclassical effects is in the third order nonlinearity, which is related to the envelope function $f(n\chi t)$, i.e. to the nonlinear phase modulation term, that causes such effects. Furthermore, involving squeezing factors, the function $f(n\chi t)$ indicates that they can exhibit collapse-revival phenomenon, as we shall see. Furthermore, the generation of squeezed light in DKNC is quite obvious from (1), which–apart from the free part–includes two main parts: linear-interaction part and self-cross nonlinear interaction part. The latter is well known in the literature, see e.g. [24], as being able to generate nonclassical light such as squeezed light, whereas the former switches energy only. Now we discuss some analytical results for the system by focusing the attention on a simple case, when $\Delta = 0s^{-1}, \alpha_1 = \alpha_2 = \alpha$. In this case expressions (13) can be written in the forms:

$$\begin{aligned} S(t) &= 2\alpha^2 + 2\alpha^2\cos[2t\lambda + \epsilon(2\chi t)]f(2\chi t) - 4\alpha^2\cos^2[t\lambda + \epsilon(\chi t)]f^2(\chi t)], \\ Q(t) &= 2\alpha^2 - 2\alpha^2\cos[2t\lambda + \epsilon(2\chi t)]f(2\chi t) - 4\alpha^2\sin^2[t\lambda + \epsilon(\chi t)]f^2(\chi t)]. \end{aligned} \tag{15}$$

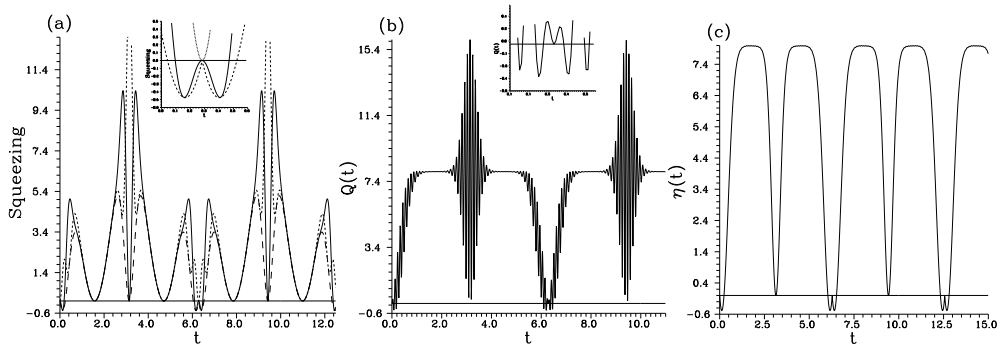

FIG. 2: Evolution of the squeezing factors and principal squeezing of the first mode when $\kappa = 1, \chi = 0.5, (\alpha_1, \alpha_2) = (2, 0)$ and for (a) $\Delta = 0s^{-1}$ (solid curve for $S(t)$, short-dashed curve for $Q(t)$ and long-dashed curve for $\eta(t)$), and $\Delta = 50s^{-1}$ for $Q(t)$ (b) and $\eta(t)$ (c). The inset in (a) shows that $Q(t)$ cannot exhibit squeezing, while that in (b) shows the amount of squeezing, which can be obtained.

It is easy to prove that

$$S(t) + Q(t) = 4\alpha^2[1 - f^2(\chi t)]. \tag{16}$$

It is evident that expressions (15) provide extreme values when the envelope functions tend to unity. This means that when the system generates squeezed light $S(t) + Q(t) \simeq 0$ and then squeezing cannot be simultaneously generated in the both the quadratures.

The envelope function in the second term of (15) is maximum when

$$\chi t = m'\pi/2, \quad m' = 1, 2, ... \tag{17}$$

In this case expressions (15) reduce to

$$\begin{aligned} S(t) &= 2\alpha^2\Big\{[1 - (-1)^{m'}] - 2[f^2(m'\tfrac{\pi}{2}) - (-1)^{m'}]\cos^2(t\lambda)\Big\}, \\ Q(t) &= 2\alpha^2\Big\{[1 - (-1)^{m'}] - 2[f^2(m'\tfrac{\pi}{2}) - (-1)^{m'}]\sin^2(t\lambda)\Big\}. \end{aligned} \tag{18}$$

From (18), for these particular values of the interaction time, it is easy to prove that squeezing occurs for weak-intensity regime, i.e. $0 < \alpha < 1$, where $f(m'\frac{\pi}{2}) \simeq 1$ for $m' = 1, 3, 5, \cdots$. Nevertheless, squeezing cannot occur for strong-intensity regime, i.e. when $\alpha > 1$ where $f(\chi t) \simeq 0$. On the other hand, the third term in (15) is maximum when

$$\chi t = m'\pi, \quad m' = 1, 2, ... \tag{19}$$

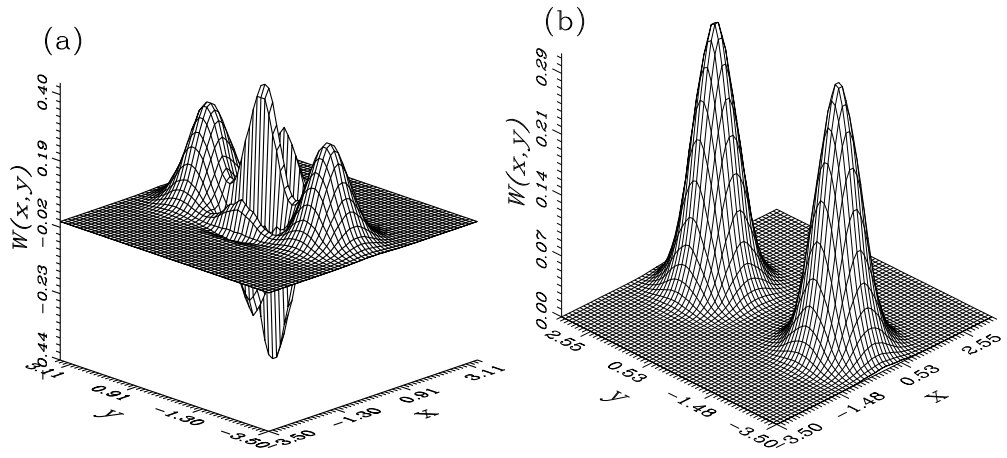

FIG. 3: The single mode W function for $\kappa = 1, \chi = 0.5, \Delta = 0s^{-1}, t = \pi$ and (a) $(\alpha_1, \alpha_2, D) = (2, 0, 0)$, (b) $(2, 2, 4)$.

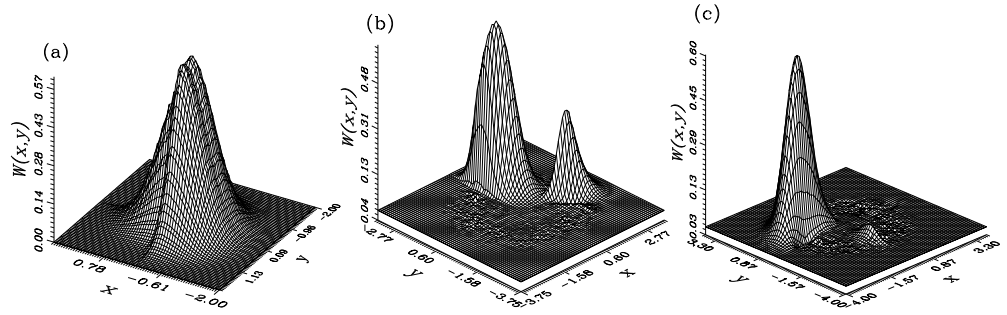

FIG. 4: The single mode W function for $\kappa = 1, \chi = 0.5$ and (a) $(\Delta, \alpha_1, \alpha_2, t) = (0s^{-1}, 0.2, 0.2, 3.139997)$, (b) $(0s^{-1}, 2, 0, 6.36005)$, (c) $(50s^{-1}, 2, 0, 6.36005)$.

In this case (15) reduces to $S(t) = Q(t) = 0$, i.e. the system generate minimum-uncertainty states. In spite of this fact we have numerically found that the system can generate squeezing close to $\chi t = m'\pi$ regardless of the values of α_j. This is related to the factor $\epsilon(n\chi t)$ involving in the trigonometric functions.

All these analytical facts and the influence of Δ on the evolution of quadrature squeezing are presented in figures 1 and 2 for given values of the parameters. From Fig. 1(a), where the intensities are weak, one can see that squeezing periodically (but not simultaneously) occurs in both the quadratures. The influence of the detuning parameter is given in Fig. 1(b), which displays an exact periodic collapse-revival phenomenon. This is related to the values of the scaled interaction time $t\lambda$, which is rapidly changed when Δ is large. More illustratively, the squeezing factors include two forms of periodic functions: one is coming

from the self-cross-nonlinear interaction part, in particular, the envelope function whose period is π/χ, and the other is arising from the linear-interaction part whose period is π/λ. Thus when the values of Δ increase, the period of the energy exchange between waveguides decreases, i.e. many oscillations occur, till the interaction time becomes $t = \pi/\chi$ at this moment the field is trapped instantaneously by nonlinearity in the waveguides and the squeezing factors show collapse. As the interaction proceeds the phenomenon is periodically repeated. Now we draw the attention to Figs. 2. From Fig. 2(a) it is obvious that the system produces vacuum and coherent light periodically. This can be realized analytically since for $\Delta = 0s^{-1}, t = (m'+1/2)\pi, \lambda = 1$ the amplitude $|\alpha_1(t)| = 0$ (regardless of the values of the χ) and the system produces the vacuum state. Similar arguments can be given for the coherent light. Also from Fig. 2(a) squeezing occurs in the $S(t)$ only (see the solid curve in the inset) at particular values of the interaction time. In fact, at these values the system generates Yurke-Stoler coherent states (YSCS) [25], as we shall show in sections 3 and 4. Moreover, squeezing can be established in $Q(t)$ when the frequency mismatch is included (see Fig. 2(b)). Also from Fig. 2(b) $Q(t)$ exhibits particular type of collapse-revival phenomenon, which can be explained in the following sense. According to the values of the interaction parameters considered in Fig. 2(b) (i.e. $\alpha_2 = 0, \Delta \gg 1s^{-1}$ and $\lambda \simeq \Delta/2$) expressions (15)–(19) and the discussion around can be used. In this regard $G_1(t)$ exhibits two times revival patterns compared to those occurring in $G_3(t)$. When revivals occur in $G_1(t)$ and $G_2(t)$ simultaneously, they destructively interfere and cancel out each others showing such shape, however, at this stage the system generates squeezing, i.e. squeezing occurs close to $\chi = m'\pi$. The comparison between figures 1(b) and 2(b) shows that as the values of α_j increase the widths (i.e. the envelopes of the revival patterns) decrease, but the collapse period is enlarged. Actually, we found that $S(t)$ provides quite similar behaviour as $Q(t)$.

Now we turn the attention to principal squeezing $\eta(t)$, which for the mode under consideration can be expressed as

$$\eta(t) = 2|\bar{\alpha}_1(t)|^2\Big\{1 - \exp[-4\varepsilon\sin^2(\chi t)] - \exp[-4\varepsilon\sin^2(\chi t)] \times \big[1 + \exp[-8\varepsilon\sin^2(\chi t)\cos(2\chi t)] - 2\exp[-4\varepsilon\sin^2(\chi t)\cos(2\chi t)]\cos[2\chi t - 4\varepsilon\sin^2(\chi t)\sin(2\chi t)]\big]^{\frac{1}{2}}\Big\}. \tag{20}$$

As we did for the quadratures squeezing one can prove that for $\chi t = m\pi$ the principal squeezing vanish, however, for $\chi t = m'\pi/2$, m' is odd integer, it reduces to

$$\eta(t) = -4|\bar{\alpha}_1(t)|^2 \exp(-4\varepsilon). \tag{21}$$

This means that squeezing always occurs provided that α_j are finite. This is related to the fact that the phase of the homodyne detector is adjusted for obtaining the minimum variance. For the resonance case principal squeezing factor $\eta(t)$ is presented by the long-dashed curves in Fig. 1(a) and Fig. 2(a) for weak and strong intensities, respectively. From Fig. 1(a) it is obvious that $\eta(t)$ provides the envelope for the periodic nonclassical effects in the $Q(t)$ and $S(t)$ factors. More precisely, $\eta(t)$ starts from zero before switching on the interaction, monotonically decreases (increasing squeezing) as the interaction time increases till $\chi t = \pi/2$ showing its minimum (maximum squeezing) and hence increases monotonically till providing its initial value at $\chi t = \pi$. This behaviour is periodically repeated. Similar behaviour has been seen for the anharmonic oscillator model [22, 23]. From Fig. 2(a) for strong intensity regime $\eta(t)$ exhibits behaviour, which is similar to that of $S(t)$. Nevertheless, $\eta(t)$ provides nonclassical squeezing over intervals of the interaction time larger than those for $S(t)$ (compare the long-dashed and solid curves in the inset). Now we draw the attention to the non-resonance case, which is presented by Fig. 2(c) for given values of the interaction parameters. We have noted that $\eta(t)$ cannot provide collapse-revival phenomenon. Moreover, for weak intensity regime $\eta(t)$ is insensitive to the value of Δ, which almost leads to the long-dashed curve in Fig. 1(a). From Fig. 2(c), which is given for strong-intensity regime, we can see that the behaviour is completely different from that of the $Q(t)$, i.e. it is periodic involving nonclassical effects (squeezing) rather than collapse-revival phenomenon. Surprisingly, Fig. 2(c) is similar to Fig. 2(e) [10] for the resonance case.

Generally, we can conclude that the origin of the occurrence squeezing and collapse-revival phenomenon in the single mode quadratures squeezing lies in the competition between the nonlinearity and the frequency mismatch. The locations of the revival patterns in the time domain depend on the values of $t\chi$ and their shapes depend on the intensities of the field launched in the waveguides initially. Finally, the behaviours of the quadrature squeezing presented here are completely different from those given in [10] as a result of neglecting the nonrelevant terms there. Also squeezing in the framework of the principal squeezing has been remarked. Nevertheless, the principal squeezing cannot exhibit collapse-revival

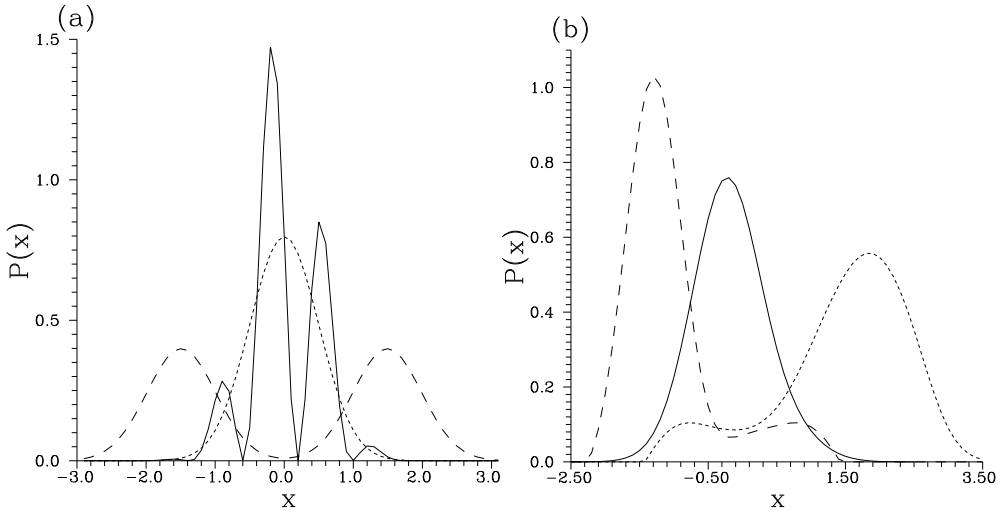

FIG. 5: The quadrature distribution $P(x)$ of the first mode for $\kappa = 1, \chi = 0.5$ and for (a) $t = \pi, \alpha_1 = 2$ and $(\alpha_2, \Delta^2, D) = (0, 0s^{-2}, 0)$ (solid curve), $(2, 0s^{-2}, 4)$ (short-dashed curve) and $(0, 5s^{-2}, 0)$ (long-dashed curve); (b) $(\Delta, \alpha_1, \alpha_2, t) = (0s^{-1}, 0.2, 0.2, 3.139997)$ (solid curve), $(0s^{-1}, 2, 0, 6.36005)$ (short-dashed curve) and $(50s^{-1}, 2, 0, 6.36005)$ (long-dashed curve).

phenomenon.

III. QUASIPROBABILITY DISTRIBUTION FUNCTION

Quasiprobability distribution functions (W-Wigner, Q-Husimi and P-Glauber functions [26]) are important tools to give insight in the statistical description of a quantum mechanical system. These functions can be measured via homodyne tomography [27]. Here we investigate the single mode quasiprobability distribution functions and quadrature distribution for the system under consideration using the technique given in [28]. Furthermore, in the following section we use these functions in investigating the phase distribution and phase variance. In order to obtain these functions we have to calculate the single mode s-parameterized characteristic function having the form

$$C(\zeta, t, s) = \mathrm{Tr}\left\{\hat{\rho}(0) \exp[\zeta \hat{A}_1^{\dagger}(t) - \zeta^* \hat{A}_1(t) + \frac{s}{2}|\zeta|^2]\right\}, \tag{22}$$

where $\hat{\rho}(0)$ is the density matrix of the system and s is a parameter that takes on the values $1, 0$ and -1 corresponding to normally, symmetrically and antinormally ordered characteristic functions, respectively. From (10) and (22) the characteristic function can be expressed as

$$C(\zeta,t,s)=\exp(\tfrac{s-1}{2}|\zeta|^2)\sum_{n_1,n_2=0}^{\infty}\tfrac{\zeta^{n_1}(-\zeta^*)^{n_2}}{n_1!n_2!}\bar{\alpha}_1^{n_2}(t)\bar{\alpha}_1^{*n_1}(t)$$
$$\times z^{[\frac{n_2}{2}(n_2-1)-\frac{n_1}{2}(n_1-1)]}\exp[\varepsilon(z^{n_2-n_1}-1)], \tag{23}$$

where we have considered that the two modes are initially prepared in coherent states with amplitudes α_1,α_2.

The s-parameterized quasiprobability functions can be obtained through the relation

$$W(\beta,t,s)=\frac{1}{\pi^2}\int C(\zeta,t,s)\exp(\beta\zeta^*-\beta^*\zeta)d^2\zeta. \tag{24}$$

On substituting (23) into (24) and using the technique given in [28] we arrive at

$$W(\beta,t,s)=\tfrac{2}{\pi(1-s)}\exp(\tfrac{-2}{1-s}|\beta|^2)\sum_{n_1,n_2=0}^{\infty}\tfrac{(-1)^{n_1}\bar{\alpha}_1^{n_2}(t)\bar{\alpha}_1^{*n_1}(t)}{n_2!}\left(\tfrac{2}{1-s}\right)^{n_2}\beta^{*n_2-n_1}$$
$$\times z^{[\frac{n_2}{2}(n_2-1)-\frac{n_1}{2}(n_1-1)]}\exp[\varepsilon(z^{n_2-n_1}-1)]\mathrm{L}_{n_1}^{n_2-n_1}\left(\tfrac{2|\beta|^2}{1-s}\right), \tag{25}$$

where $\mathrm{L}_n^m(.)$ is the associated Laguerre polynomial of order n and $\beta=x+iy=|\beta|\exp(i\Theta)$, Θ being the phase of β. One can easily verify that when $\chi t=m'\pi$ and m' is integer, the system produces coherent light with amplitude $\bar{\alpha}_1(t)$, as we mentioned in section 2. This can be verified from (25) by means of the generating function for the Leguerre polynomials (see (47) in the Appendix). In this case (25) reduces to the W function for the coherent state

$$W(\beta,t,s)=\frac{2}{\pi(1-s)}\exp\left[-\frac{2}{1-s}|\beta-\bar{\alpha}_1(t)|^2\right]. \tag{26}$$

Furthermore, (26) indicates that the distribution cannot provide negative values at the phase space origin, i.e. $\beta=0$. Generally, (25) includes complicated quadratic phase factor, which plays an essential role in generating cat states [29] and it reflects the strong entanglement between the two modes. In fact, for particular values of the parameter $t\chi$ expression (25) can reduce to that for the cat states. For instance, when $t\chi=(m'+1/2)\pi$ and m' is integer, (25) can be modified to the following form:

$$W(\beta,t,s)=\tfrac{1}{\pi(1-s)}\Big\{\exp\left(-\tfrac{2}{1-s}|\beta-i\bar{\alpha}_1(t)|^2\right)+\exp\left(-\tfrac{2}{1-s}|\beta+i\bar{\alpha}_1(t)|^2\right)$$
$$+2\exp\left[-\tfrac{2}{1-s}(|\beta|^2+D)\right]\sin\left(\tfrac{2}{1-s}(\beta\bar{\alpha}_1^*(t)+\beta^*\bar{\alpha}_1(t))\right)\Big\}, \tag{27}$$

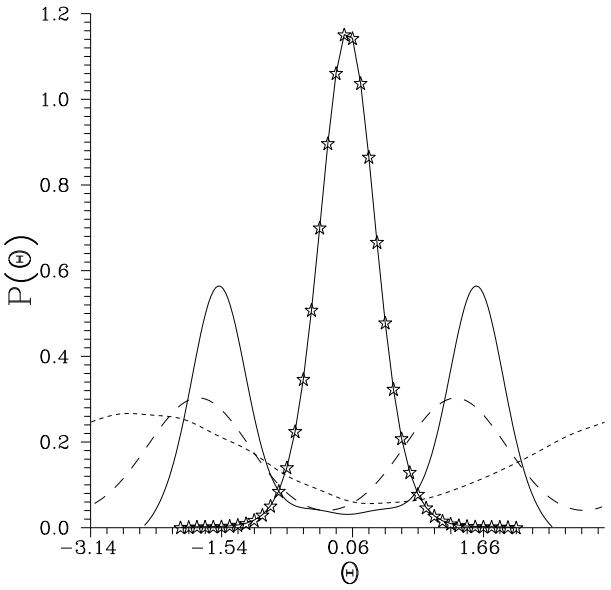

FIG. 6: The single mode phase distribution $P(\Theta, t, s = -1)$ for $\kappa = 1, \chi = 0.5, (\Delta, \alpha_1, \alpha_2) = (0s^{-1}, 2, 2)$ and for $t = 0$ (star-centered curve), $\pi/4$ (short-dashed curve), 2.94 (long-dashed curve) and π (solid curve).

where

$$D = \varepsilon - |\bar{\alpha}_1(t)|^2. \tag{28}$$

The derivation of (27) is given in the Appendix. Moreover, one can easily verify that (27) is normalized,

$$\int W(\beta, t, s) d^2\beta = 1. \tag{29}$$

The form (27) reduces to that of YSCS [25] when $D \simeq 0$. In other words, when $D \simeq 0$ the system generates the states

$$|\psi(t)\rangle = \frac{1}{\sqrt{2}}[|i\bar{\alpha}_1(t)\rangle + \exp(i\frac{\pi}{2})| - i\bar{\alpha}_1(t)\rangle], \tag{30}$$

which is YSCS. As is well known YSCS exhibit Poissonian statistics and provide squeezing [30]. These results are obtained in section 2. This indicates that the cat states generated in DKNC are YSCS. Moreover, when $\Delta = 0s^{-1}$ and from (12), expression (28) takes the form

$$D = \alpha_1^2 \sin^2(\lambda t) + \alpha_2^2 \cos^2(\lambda t). \tag{31}$$

Expression (31) provides several consequences: (i) DKNC generates YSCS when one of the modes is initially prepared in the vacuum state and the other is in the coherent state

provided that the length of the waveguides (or the interaction time) is controlled so that $D = 0$. (ii) when $\lambda = 0$, i.e. the linear interaction between the waveguides is neglected, the system can generate YSCS by choosing $\alpha_1 \neq 0$ and $\alpha_2 = 0$. (iii) the system cannot generate YSCS when $\alpha_1 = \alpha_2 = 0$ even though $D = 0$, because the expression (27) reduces to that for the vacuum.

On the other hand, when $D \geq 1$ the interference part in (27) is destroyed and hence the DKNC generates the statistical-mixture coherent states having the form

$$\hat{\rho}(t) = \frac{1}{2}\left[|i\bar{\alpha}_1(t)\rangle\langle i\bar{\alpha}_1(t)| + |-i\bar{\alpha}_1(t)\rangle\langle -i\bar{\alpha}_1(t)|\right]. \tag{32}$$

An illustration of (27) (or (25)) is given in Figs. 3(a) and (b) for $D = 0$ and 4, respectively. In Fig. 3(a) the W function consists of two Gaussian bells, corresponding to the statistical mixture of individual composite states (cf. (30)) and interference fringes inbetween arising as a result of the contribution originating from the quantum superposition. In Fig. 3(b) the interference fringes are completely suppressed and the form of the statistical-mixture coherent states is well pronounced. Actually, by controlling the values of the Δ, the form of the cat states can be less or more pronounced. For instance, Fig. 3(a) can be reduced to Fig. 3(b) by taking $\Delta = \sqrt{5}s^{-1}$ instead of zero.

Now we shed the light on the general case, e.g. apart from the case $t\chi = (m' + 1/2)\pi$. This will be numerically done by figures 4 for the W function obtained from (25). The values of the interaction parameters in Figs. 4 have been selected such that the system provides quadratures squeezing (see Figs. 1 and 2). In all these figures we can observe the nonclassical effects, such as negative values, stretching, multipeak structure and deformation. In Fig. 4(a), where the initial intensities of the modes are weak, the W function exhibits contour-stretching as well as deformation around the phase space origin. The origin of such behaviour is in the generation of cat states in the microscopic regime [28], where the contribution of the different components of the cat are located close to the phase space origin competing each others. When the values of the intensities and the value of the interaction time are increased, the shape of the cat states becomes more pronounced by involving multipeak structure (asymmetric peaks) (see Fig. 4(b)). This is in a good agreement with the information given above even though $t\chi \neq (m' + 1/2)\pi$. We proceed by drawing the attention to the influence of the detuning parameter on the behaviour of the W function, which is given in Fig. 4(c). In this figure the W function exhibits almost stretched single peak structure

as well as negative values indicating that the nonclassical effects are still occurring. The transition from Fig. 4(b) to Fig. 4(c) through changing the values of the detuning is related to the fact that in the former the amplitude $\bar{\alpha}_1(t)$ is real, while in the latter it is complex (one can check this for the chosen values of the interaction parameters). This leads to that the oscillations arising from the nonlinear phase modulation are superimposed with those of the field amplitude $\bar{\alpha}_1(t)$ causing such behaviour in Fig. 4(c). We conclude this part by mentioning that a connection between the Fourier coefficients and the Q function for the case $2\chi = \bar{\chi}$ using the diagonalization approach is given in [12].

We close this section by investigating the quadrature (or position) distribution $P(x,t)$, which can be measured in the homodyne detector [25]. The distribution $P(x,t)$ can be evaluated via the W function through the relation

$$P(x,t) = \int_{-\infty}^{\infty} W(x+iy,t,0)dy. \tag{33}$$

Substituting (25) into (33) and after lengthy calculation, we arrive at

$$\begin{aligned} P(x,t) = \sqrt{\tfrac{2}{\pi}}\exp(-2x^2) \sum_{n_1,n_2=0}^{\infty} \sum_{r=0}^{min(n_1,n_2)} \tfrac{(-2)^r 2^{-\frac{1}{2}(n_1+n_2)} \bar{\alpha}_1^{n_2}(t)\bar{\alpha}_1^{*n_1}(t)}{r!(n_1-r)!(n_2-r)!} \\ \times z^{[\frac{n_2}{2}(n_2-1)-\frac{n_1}{2}(n_1-1)]} \exp[\varepsilon(z^{n_2-n_1}-1)] \mathrm{H}_{n_1-r}(\sqrt{2}x)\mathrm{H}_{n_2-r}(\sqrt{2}x), \end{aligned} \tag{34}$$

where $\mathrm{H}_m(.)$ is the Hermite polynomial of order m. It is more convenient to give the explicit form for $P(x,t)$ for the case $t\chi = (m'+1/2)\pi$

$$\begin{aligned} P(x,t) = \tfrac{1}{\sqrt{2\pi}}\Big\{ \exp[-2(x+\bar{\alpha}_y(t))^2] + \exp[-2(x-\bar{\alpha}_y(t))^2] \\ +2\exp[-2(x^2+\bar{\alpha}_y^2(t)+D)]\sin(4x\bar{\alpha}_x(t))\Big\}. \end{aligned} \tag{35}$$

In Figs. 5(a) and (b) we have plotted $P(x,t)$ corresponding to the W functions shown in Figs. 3 and 4, respectively. In general one can observe that $P(x,t)$ provides nonclassical effects by including oscillatory behaviour. In Fig. 5(a) the solid curve shows the oscillatory behaviour related to YSCS, which is a direct consequence of the interference in phase space. Nevertheless, the short-dashed curve is a Gaussian bell having its maximum value at $x = 0$. This indicates that the system generates vacuum light. Actually, for this curve $\bar{\alpha}_y(t) \simeq 0$ and the interference part is completely suppressed since $D = 4$. This may contradict to the

result illustrated in Fig. 3(b) for the corresponding W function, in which the generation of the statistical-mixture coherent state is obvious. This confusion can be removed if the attention is drawn to the momentum distribution $P(y,t)$, which exhibits, for this case, a two-peak structure (we have checked this fact). The influence of the Δ is presented by the long-dashed curve, which provides the two-peak structure indicating the generation of the statistical-mixture coherent state. On the other hand, we can note that there is almost consistence between the behaviours in Figs. 4 and Fig. 5b, where $P(x,t)$ provides two asymmetric peaks for strong intensities regardless of the values of Δ and a single peak for weak intensities. We conclude this section by mentioning in [31] stated that "the concept of interference in phase space readily explains the similarity between the photon number distribution and the position distribution". This is not always correct. For instance, $P(x,t)$ of the YSCS provides oscillatory behaviour (see the solid curve in Fig. 5(a)) even though the photon number distribution of YSCS is Poissonian, as we mentioned in section 2.

IV. PHASE DISTRIBUTION AND ITS VARIANCE

In this section we study the evolution of the phase distribution and its variance. The phase distribution associated with the first mode can be obtained from the quasidistribution (25) by integrating $W(\beta,t,s)$ over the radial variable as

$$P(\Theta,t,s)=\int_0^\infty |\beta| W(\beta,t,s) d|\beta|. \tag{36}$$

On substituting (25) into (36) and carrying out the integration, we arrive at

$$\begin{aligned} P(\Theta,t,s)=\tfrac{1}{2\pi}\Big\{1+2\sum_{n_2>n_1}^{\infty}\sum_{m=0}^{n_1}\tfrac{(-1)^{n_1+m}\Gamma(m+\frac{n_2-n_1}{2}+1)|\bar\alpha_1(t)|^{n_2+n_1}}{(n_1-m)!(n_2-n_1+m)!m!}\left(\tfrac{2}{1-s}\right)^{\frac{n_1+n_2}{2}} \\ \times\cos[\varphi+(n_1-n_2)\Theta]\exp[-2\varepsilon\sin^2((n_2-n_1)\chi t)]\Big\}, \end{aligned} \tag{37}$$

where

$$\begin{aligned} \bar\alpha_1(t)&=|\bar\alpha_1(t)|\exp[i\bar\phi(t)], \\ \varphi&=(n_2-n_1)\bar\phi(t)+[n_2(n_2-1)-n_1(n_1-1)]\chi t+\varepsilon\sin(2\chi t(n_2-n_1)) \end{aligned} \tag{38}$$

and $\Gamma(.)$ is the Gamma function. The phase distribution given by (37) is just a special case of the formula (2.59) in [32]. As is well known the phase distribution obtained from the

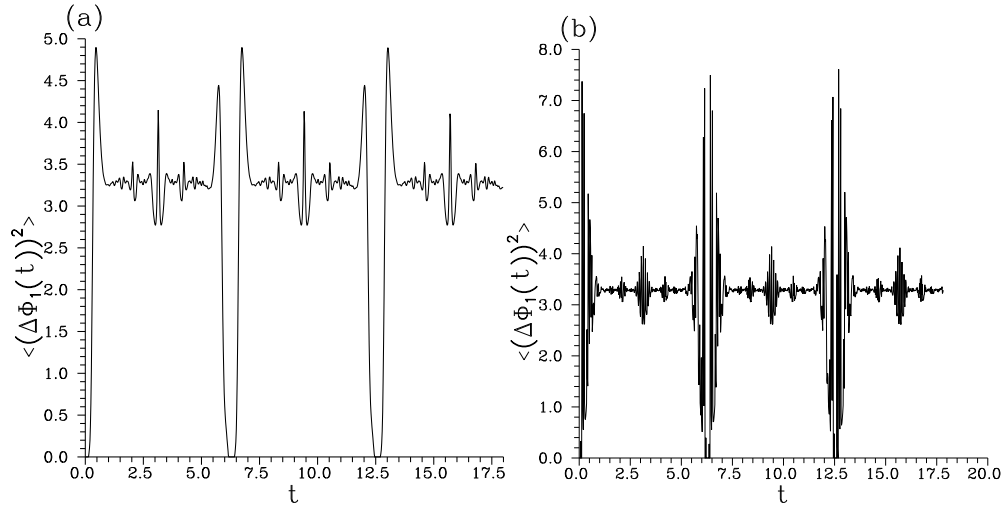

FIG. 7: The single mode phase variance $\langle(\triangle\Phi_1(t))^2\rangle$ against the interaction time t for $\kappa = 1, \chi = 0.5$ and (a) $(\Delta, \alpha_1, \alpha_2) = (0s^{-1}, 2, 2)$ and (b) $(50s^{-1}, 2, 2)$.

quasiprobability distribution functions includes some difficulties. For instance, the singularity of the P function and the negative values involved in the W function for some quantum mechanical systems may be reflected in the corresponding phase distributions (see, e.g., [33]). These difficulties can be avoided by using Q function, which is well defined and is always positive, in evaluating the phase distribution. Illustration of $P(\Theta, t, s = -1)$ is given in Fig. 6 for given values of the parameters. From this figure one can see how the cat states can be generated in the system depending on the values of the interaction time (or the length of the waveguides). For instance, at $t = 0$, i.e. before switching on the interaction, $P(\Theta)$ exhibits single-peak structure around $\Theta = 0$, which is representative for the coherent light (see the star-centered curve). As the interaction proceeds, i.e. energy exchange between the waveguides starts to play a role, the initial peak reduces to two wings around $\Theta = \pm\pi$, which becomes straight line at $t\chi = \pi/2$, i.e. the phase distribution exhibits normal distribution (this case has not been included in the figure). It is worth remembering that the system generates vacuum state in this case. When the interaction time becomes close to π the form of the cat states starts to appear as a broader two-peak structure (see the long-dashed curve in Fig. 6). Eventually, at $t = \pi$ the distribution provides two Gaussian peaks around $\Theta = \pm\pi/2$ indicating the generation of the cat state, in particular, the statistical-mixture coherent state (cf. (32)). Actually, the phase distribution is insensitive to the interference in phase space, i.e. the phase distribution of the even, odd, Yurke-Stoler

and the statistical-mixture coherent states are almost similar [34]. This leads to the fact that the phase distribution is insensitive to the values of Δ, which can change cat states to the statistical-mixture coherent states (see the discussion given in section 3 for the W function).

The single mode phase variance is defined as

$$\langle(\triangle\hat{\Phi}_1(t))^2\rangle = \langle\hat{\Phi}_1^2(t)\rangle - \langle\hat{\Phi}_1(t)\rangle^2. \tag{39}$$

The lth moment of the phase distribution can be evaluated from (37) through the relation

$$\langle\hat{\Phi}_1^l(t)\rangle = \int_{-\pi}^{\pi} \Theta^l P(\Theta, t, s) d\Theta. \tag{40}$$

The evolution of the $\langle(\triangle\hat{\Phi}_1(t))^2\rangle$ is given in Figs. 7(a) and (b) for $\Delta = 0s^{-1}$ and $50s^{-1}$, respectively. In Fig. 7(a) the periodic behaviour is dominant indicating switching of energy between the waveguides. Also one can see that the system provides its initial stage periodically. The detuning parameter Δ reflects itself in $\langle(\triangle\hat{\Phi}_1(t))^2\rangle$ as collapse-revival-subrevival phenomenon (see Fig. 7(b)). As we mentioned in section 2, when the values of the Δ increase, the period of switching of energy between the waveguides decreases, causing such phenomenon. Furthermore, the main revivals occur around the values of the interaction times at which the system reduces to its initial form, however, the subrevivals occur when the system generate cat states. Actually, the density matrix of the superposition states has different components, each of them has its own collapse-revival pattern (when Δ is large), which interfere with each others producing subrevivals. Thus we can conclude that the occurrence of the collapse-revival-subrevival phenomenon is a direct consequence of the generation of different types of states in the system, i.e. vacuum, coherent, and cat states. It is worth mentioning that such behaviour has been observed for the single mode phase variance of the two-mode Jaynes-Cummings model [17], however, the behaviour presented here is more systemic.

V. CONCLUSION

In this paper we have discussed the single mode quantum properties for the codirectional nonlinear Kerr coupler, when the frequency mismatch is involved. The attention is

focused on the case $2\chi = \widetilde{\chi}$ for which the solutions of the equations of motion are exact. We have investigated quadratures squeezing, principal squeezing, quasiprobability distribution functions, quadrature distribution, phase distribution and phase variances. Generally, we have shown that the light obtained from the system exhibits Poissonian statistics and provides squeezing in the framework of quadratures and principal squeezing. Moreover, it has been shown that when the values of Δ increase the period of the energy exchange between waveguides decreases. This fact leads to many interesting effects, such as the quadratures squeezing and the phase variances can exhibit collapse-revival and collapse-revival-subrevival phenomena, respectively. The generation of YSCS in the system has been analytically and numerically demonstrated and confirmed in all studied quantities. YSCS can be generated even if the linear interaction between the waveguides is neglected. Moreover, we have shown that the generation of these states most probably occurs when initially one of the modes is in the coherent state while the other is in vacuum state, provided that $t\chi = N\pi$ and N is a fraction of integer. Furthermore, the system can generate the statistical-mixture coherent states in dependence on the values of the interaction parameters. The nonclassical effects have been remarked in the behaviour of $P(x,t)$. Finally, $P(x,t)$ cannot include a complete information on the interference in phase space.

Appendix

In this appendix we give the derivation of the quasiprobability distribution given by (27). It is worth reminding that $t\chi = (m' + 1/2)\pi$, i.e. $z = -1$. We start by providing the following array:

$$\begin{aligned} n_1 &= 1, 2, 3, 4, 5, 6, 7, 8, \cdots \\ l = \frac{n_1}{2}(n_1 - 1) &= 0, 0, 1, 3, 6, 10, 15, 21, \cdots \\ z^l &= 1, 1, -1, -1, 1, 1, -1, -1, \cdots \end{aligned} \tag{41}$$

From the information shown in (41) we can express the summation associated with the index n_1 in (25) (for this case) as

$$W(\beta, t\chi, s) = \sum_{n_1,n_2} (-1)^{n_1} z^{-\frac{n_2}{2}(n_2-1)} [h(2n_1 - n_2)F(2n_1, n_2) - h(2n_1 + 1 - n_2)F(2n_1 + 1, n_2)], \tag{42}$$

where

$$F(n_1,n_2)=\frac{2}{\pi(1-s)}\exp\left(\frac{-2}{1-s}|\beta|^2\right)\frac{\bar{\alpha}_1^{n_2}(t)\bar{\alpha}_1^{*n_1}(t)}{n_2!}\left(\frac{2}{1-s}\right)^{n_2}\beta^{*n_2-n_1}\mathrm{L}_{n_1}^{n_2-n_1}\left(\frac{2|\beta|^2}{1-s}\right), \tag{43}$$

$$h(n_1-n_2)=\exp[\varepsilon(z^{n_2-n_1}-1)]. \tag{44}$$

It is evident that, for these specified values of $t\chi$, when n_1-n_2 is even $h(n_1-n_2)=1$ otherwise $h(n_1-n_2)=\exp(-2\varepsilon)$. Moreover, the summation related to n_2 in (42) can be similarly expressed as that over n_1 and hence (42) takes the form

$$\begin{aligned}W(\beta,t\chi,s)=&\sum_{n_1,n_2}(-1)^{(n_1+n_2)}\\&\Big\{F(2n_1,2n_2)-F(2n_1+1,2n_2+1)\\&+\exp[-2\varepsilon][F(2n_1,2n_2+1)-F(2n_1+1,2n_2)]\Big\}.\end{aligned} \tag{45}$$

Now we show how the first summation can be evaluated in a closed form:

$$\sum_{n_1,n_2}(-1)^{(n_1+n_2)}F(2n_1,2n_2)=\frac{1}{4}\sum_{n_1,n_2}(i)^{(n_1+n_2)}[1+(-1)^{n_1}][1+(-1)^{n_2}]F(n_1,n_2). \tag{46}$$

Substitute (43) into (46) and use the generating function for the Laguerre polynomials [35] as

$$\exp(-xk)(1+k)^{\nu}=\sum_n k^n\mathrm{L}_n^{\nu-n}(x). \tag{47}$$

Therefore, the summation related to the index n_1 in (46) can be easily carried out and we obtain

$$\begin{aligned}\sum_{n_1,n_2}(-1)^{(n_1+n_2)}F(2n_1,2n_2)=&\tfrac{1}{2\pi(1-s)}\sum_{n_2}\frac{\left[\frac{2i\bar{\alpha}_1(t)\beta^*}{(1-s)}\right]^{n_2}}{n_2!}[1+(-1)^{n_2}]\Big\{[1+\tfrac{i\bar{\alpha}_1^*(t)}{\beta^*}]^{n_2}\\&\times\exp\left(-\tfrac{2i\bar{\alpha}_1^*(t)\beta}{1-s}\right)+[1-\tfrac{i\bar{\alpha}_1^*(t)}{\beta^*}]^{n_2}\exp\left(\tfrac{2i\bar{\alpha}_1^*(t)\beta}{1-s}\right)\Big\}.\end{aligned} \tag{48}$$

Now the summation over n_2 can be straightforwardly evaluated and we obtain the following closed form expression:

$$\sum_{n_1,n_2}(-1)^{(n_1+n_2)}F(2n_1,2n_2)=\frac{1}{2\pi(1-s)}\Big\{\exp\left(-\tfrac{2}{1-s}|\beta-i\bar{\alpha}_1(t)|^2\right)+\exp\left(-\tfrac{2}{1-s}|\beta+i\bar{\alpha}_1(t)|^2\right) \tag{49}$$

$$+2\exp\left[-\tfrac{2}{1-s}(|\beta|^2-|\bar{\alpha}_1(t)|^2)\right]\cos\left(\tfrac{2}{1-s}(\beta\bar{\alpha}_1^*(t)+\beta^*\bar{\alpha}_1(t))\right)\Big\}.$$

Similar procedures have to be performed to obtain the other terms in (45) and then (27) is obtained.

Acknowledgement

J.P. thanks the partial support from the grant LN00A015 of the Czech Ministry of Education and from the EU Project COST OCP 11.003.

References

[1] Ekert A and Jozsa R 1996 *Rev. Mod. Phys.* **68** 733; Lo H-K, Popescu S and Spiller T 1998 "*Introduction to Quantum Computation and Information*" (World Scientific: Singapore); Begie A, Braun D, Tregenna B and Knight P L 2000 *Phys. Rev. Lett.* **85** 1762.

[2] Peřina Jr J and Peřina J 2000 *Progress in Optics* **41**, ed. E. Wolf (Amsterdam: Elsevier), p. 361; Fiurášek J and Peřina J 2001 *Coherence and Statistics of Photons and Atoms*, ed. J. Peřina (New York: J. Wiley), p. 65.

[3] Li Kamwa P, Stitch J E, Mason N J and Roberts P N 1985 *Electron. Lett.* **21** 26; Jin R, Chuang C L, Gibbs H H, Koch S W, Polky J N and Pubanz G A 1986 *Appl. Phys. Lett.* **49** 110.

[4] Gusovkii D D, Dianov E M, Mairer A A, Neustreuev V B, Shklovskii E I and Scherbakov I A 1985 *Sov. J. Quant. Electron.* **15** 1523.

[5] Townsend P D, Baker G L, Shelburne J L III and Etemad S 1989 *Proc. SPIE* **1147** 256.

[6] Jensen S M 1982 *IEE J. Quant. Electron. QE* **18** 1580.

[7] Chefles A and Barnett S M 1996 *J. Mod. Opt.* **43** 709.

[8] Horák R, Bertolotti M, Sibilia and Peřina J 1989 *Opt. Soc. Am. B* **6** 199.

[9] Peřina J, Horák R, Hradil Z, Sibilia C and Bertolotti M 1989 *J. Mod. Opt.* **36** 571.

[10] Korolkova N and Peřina J 1997 *Opt. Commun.* **136** 135.

[11] Korolkova N and Peřina J 1997 *J. Mod. Opt.* **44** 1525.

[12] Fiurášek J, Křepelka J and Peřina J 1999 *Opt. Commun.* **167** 115.

[13] Ibrahim A-B M A, Umarov B A and Wahiddin M R B 2000*Phys. Rev. A* 61 043804.

[14] Ariunbold G and Peřina J 2000 *Opt. Commun.* **176** 149.

[15] Ariunbold G and Peřina J 2000 2001 *J. Mod. Opt.* **48** 1005.

[16] Jaynes E T and Cummings F W 1963 Proc. IEEE **51** 89.

[17] El-Orany F A A, Mahran M H, Wahiddin R B and Hashim A B 2004 *Opt. Commun.* **240** 169.

[18] Peřinová V, Lukš A, Křepelka J, Sibilia C and Bertolotti M 1991 *J. Mod. Opt.* **38** 2429.

[19] Peřina J and Peřina Jr J 1995 *Quant. Semiclass. Opt.* **7** 863.

[20] Fiurášek J and Peřina J 1999 *J. Mod. Opt.* **46** 1255.

[21] Braunstein S L and Kimble H J 1998 *Phys. Rev. Lett.* **80** 869; Milburn G J and Braunstein S L 1999 *Phys. Rev. A*. **60** 937; Ralph T C 2000 *Phys. Rev. A* **61** 010303(R); Hillery M 2000 *Phys. Rev. A* **61** 022309.

[22] Lukš A, Peřinová V and Hradil Z 1988 *Act. Phys. Pol.* **74** 713.

[23] Tanaś R, Miranowicz A and Kielich S 1991 *Phys. Rev. A***43** 4014.

[24] Bužek V 1989 *Phys. Lett. A* **136** 188.

[25] Yurke B and Stoler D 1986 *Phys. Rev. Lett.* **57** 13.

[26] Wigner E 1932 *Phys. Rev.* **40** 749; Cahill K E and Glauber R J 1969 *Phys. Rev.* **177** 1882; Hillery M, O'Connell R F, Scully M O and Winger E P 1984 *Phys. Rep.* **106** 121.

[27] Beck M, Smithey D T and Raymer M G 1993 *Phys. Rev. A* **48** 890; Smithey D T, Beck M, Cooper J and Raymer M G 1993 *Phys. Rev. A* **48** 3159; Beck M, Smithey D T, Cooper J and Raymer M G 1993 *Opt. Lett.* **18** 1259; Smithey D T, Beck M, Cooper J, Raymer M G and Faridani M B A 1993 *Phys. Scr. T* **48** 35; Leonhardt U 1997 "*Measuring the Quantum State of Light*" (University Press: Cambridge).

[28] El-Orany F A A 2002 *Phys. Rev. A* **65** 043814.

[29] Miranowicz A, Tanaś R and Kielich S 1990 *Quant. Opt.* **2** 253; Miranowicz A, Tanaś R, Gantsog Ts and Kielich S 1991 *J. Opt. Soc. Am. B* **8** 1576.

[30] El-Orany F A A 1999 *Czech. J. Phys.* **49** 1145.

[31] Schleich W, Pernigo M and Kien F L 1991 *Phys. Rev. A* **44** 2172.

[32] Tanaś R, Miranowicz A and Gantsog Ts 1996 *Progress in Optics* **35**, ed. E. Wolf (Amsterdam: Elsevier), p. 355.

[33] See the special issue of *Physica Scripta* 1993 **T48**.

[34] Bužek V, Gantsog Ts and Kim M S 1993 *Phys. Scr.* **48** 131.

[35] Gradshteyn I S G and Ryzhik I M 1994 *"Table of Integrals, Series, and Products"* (Boston: Academic).